IOP Conference Series: Materials Science and Engineering

Synthesis of $Bi_2Fe_xNbO_7$ films applied as a catalyst for hydrogen production using visible-light photo-electrolysis

IOP Conf. Series: Materials Science and Engineering **659** (2019) 012081 doi:10.1088/1757-899X/659/1/012081

Synthesis of $Bi_2Fe_xNbO_7$ films applied as a catalyst for hydrogen production using visible-light photo-electrolysis

A R A Scharnberg[1], A Pavlovic[2] and A K Alves[1]

[1] Laboratory of Ceramic Materials, Department of Materials, Federal University of Rio Grande do Sul - UFRGS, Osvaldo Aranha 99, Porto Alegre, RS 90035-190, Brazil
[2] Interdepartmental Center for Industrial Research on Advanced Mechanics and Materials, University of Bologna, Viale del Risorgimento 2, 40136, Bologna, Italy

E-mail: allan.ambiental@outlook.com

Abstract. The seek for feasible sustainable mobility alternatives is a major concern of the society nowadays. By its turn, the production of hydrogen represents one of the main lines of study on clean energy, since hydrogen presents the possibility of storage and association with other renewable energy sources. In this regard, photo-electrolysis is a promising option for hydrogen generation. This process optimizes the electrolysis of water by using external energy to increase the potential of a photo-electrode, which must be a material that absorbs sunlight (usually a semiconductor activated by solar radiation), promoting the generation of H_2 at the cathode. Titanium dioxide (TiO_2) is the most applied semiconductor in photocatalytic applications. However, the band gap of this material limits its activity only under UV light, disregarding about 90% of incident solar radiation. Researchers explore catalysts that can be activated under visible light, such as bismuth-based mixed oxide semiconductors, which have attracted interest because of their excellent stability, visible light absorption, and photocatalytic properties. This research aims to develop and characterize photo-anodes based on bismuth, niobium and iron oxides ($Bi_2Fe_xNbO_7$), for production of hydrogen via photo-electrolysis of water. The films were produced by the sol-gel process and deposited under a conductive glass slide by dip-coating. The effect of the iron concentration was evaluated by UV-Vis spectroscopy and SEM analysis, in order to estimate its hydrogen production potential.

1. Introduction

Since the beginning of time, the advances of our civilization are confused with technological advances [1]. Before the industrial revolution, the main source of energy was biomass, like firewood. After that, with the invention of the steam engine, the natural coal gradually replaced the firewood. After World War II, due to the development of the automobile industry and the emergence of multinational oil companies, oil consumption has grown exponentially: since the beginning of the 21st century, oil, coal and natural gas are the three main sources of global supply of energy, accounting for over 80% of all consumption [2]. Accompanying the trends of economic, technological and population growth, global energy demand has been growing continuously. As most of this energy matrix is composed of fossil fuels, this growth has given rise to a series of environmental problems, mainly due to the emission of greenhouse gases (GHG).

Carbon dioxide emissions from fossil fuels have increased the average concentration of CO_2 in the atmosphere from 270 to 400 ppm in the last 110 years and is estimated that the level reaches 600 ppm by 2050 [3]. This phenomenon can lead to glacier melting, rising and acidification of the ocean, coral extinction, epidemics of temperature-making diseases, tropical storms and extreme snowstorms [4]. Besides, fossil reserves are finite [5], subject to geopolitical conflicts, and there are more noble applications for them, such as the petrochemical industry. Due to these facts, there is a need to develop new technologies for energy generation.

In recent decades there has been a significant development of non-fossil energy sources, such as solar, wind, geothermal and nuclear [2], which has contributed to the reduction of GHG emissions. The challenge is to find a source of energy that is abundant, emission-free and sustainable. Representing a major cause of pollutant emissions, research on urban mobility has seek to take advantage of the solar energy to produce innovative, safe, lightweight and zero-emission vehicles [6–8], although the energy efficiency of these vehicles, using a photovoltaic technology, still has room for improvement.

One of the most interesting proposals to attain that goal is the photo-electrolysis, which also consists in the usage of the solar energy, but to produce hydrogen, since it presents the possibility of storage and association with other renewable sources of energy [3]. In order for hydrogen to be considered a truly emissions-free fuel, its only byproduct must be water, and its entire production process must be carried out cleanly. The most commonly used process for hydrogen production today is from the reform of methane to steam, which cannot be considered a clean process.

Photo-electrolysis is a process similar to electrolysis, but it makes direct use of light by the conversion of solar light into electrical current and then the transformation of water into useful chemical energy (H_2). A photo-electrolytic cell (PEC) is composed of a semiconductor device that absorbs solar energy and generates the voltage necessary to separate the water molecules as shown in figure 1. Photo-electrolysis integrates the generation of solar energy and electrolysis of water in a single photo-anode and is considered the most promising renewable method for hydrogen production [9]. Figure 2 demonstrate de reaction mechanism in the surface of the semiconductor photo-anode.

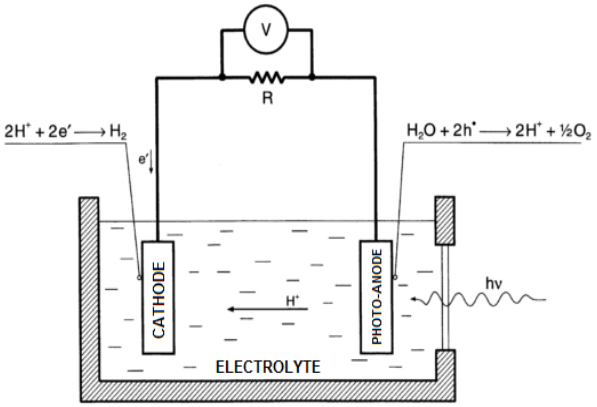

Figure 1. Structure of a photo-electrochemical cell (PEC) for water photo-electrolysis. Adapted from Bak et al, 2002 [10].

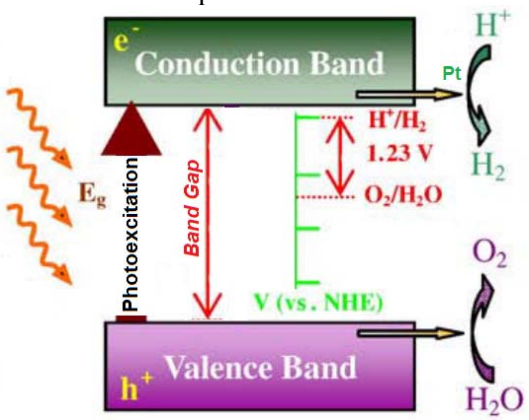

Figure 2. The principle diagram for photo-catalytic water splitting on a semiconductor. Adapted from Zhu et al, 2009 [11].

This technique has begun in 1972 when companies [12] used titanium oxide as the electrode for the production of hydrogen in a photo-electrochemical cell. Several studies have pointed out oxides with possible relevance for use in this process; many of them present difficulties as cost, obtaining and toxicity. The semiconductor must have a short band gap value to absorb a large part of visible light irradiation [13]. Therefore, ideal semiconductor materials for PEC application must have a low band gap, be stable in operation, permit electron mobility, do not show high electron/hole recombination capacity, be affordable and available [14].

Researchers explore catalysts that can be activated under visible light, such as coupled semiconductors, doped semiconductors and mixed metal oxide semiconductors, such as bismuth-based mixed oxide semiconductors, which have attracted interest because of their excellent stability, visible light absorption and photocatalytic properties. These include, among others, bismuth oxide (Bi_2O_3), bismuth niobate (Bi_3NbO_7), bismuth ferrite ($Bi_2Fe_4O_9$), perovskite bismuth ferrite (BiFeO), and mixed iron, bismuth and niobium oxides (Bi_2FeNbO_7) [11,15–19]. In this research, with the intention of developing photocatalysts based on bismuth, iron and niobium oxides for hydrogen production via photo-electrolysis of water, thin films were synthesized and characterized regarding their morphology and optical properties.

2. Experimental details

In order to develop and characterize photo-anodes based on bismuth, niobium and iron ($Bi_2Fe_xNbO_7$) for hydrogen production by photo-electrolysis of water, films were synthesized by the sol-gel method and deposited by dip coating on fluorine-doped SnO_2 (FTO) glass substrates. Four compositions were proposed, one without iron (Bi_2NbO_7) and with 0.8, 1.0 and 1.2 mole of iron ($Bi_2Fe_{0.8}NbO_7$; Bi_2FeNbO_7 and $Bi_2Fe_{1.2}NbO_7$), in order to evaluate its influence of iron concentration on the photocatalytic activity of the films.

The films were prepared in three steps: a) dissolution of the stoichiometric amounts of metal precursor ($Fe(NO_3)_3.9H_2O$/Synth) in 5 ml of Acetylacetone (Sigma-Aldrich) under magnetic stirring for 15 minutes. Parallel to this process, stoichiometric quantities of ($Bi(NO_3)_3.5H_2O$/Vetec) were solubilized in 5 ml of Acetylacetone under magnetic stirring for 15 minutes. Niobium chloride ($NbCl_5$) was solubilized in 4 ml of hydrochloric acid under magnetic stirring for 5 minutes. 2) After total solubilisation of both, the solution containing bismuth was homogenized, with agitation, with the solution containing iron. 3) Then, the niobium containing solution was titrated to the above, kept under constant stirring until complete homogenization, forming a uniform sol with orange-yellow coloration.

For the preparation of the films by the dip coating process, a universal machine of mechanical tests was used. FTO glass slides (15mm×25mm) were used as substrate for deposition of the sol and support for the thin films. They were previously cleaned with ethanol in the bath for 30 minutes. Five immersions were performed for each slide, with a 5 minute interval between each to dry the deposited material. The settling speed was set at 5 cm min^{-1}, as it conferred good uniformity to the deposited layers at each stage. After the dip coating process, the samples were dried at room temperature for 15 hours. Subsequently, they were heat-treated at 600°C. A slow heating rate (2°C min^{-1}) and 1h maximum temperature was used to produce thin films with good crystallinity.

2.1. Characterizations

In the area of catalytic materials for photo-electrolysis, it is essential to obtain information about the band gap value of the material, thus confirming the minimum energy size for the water splitting reaction, as well as the capacity of the material to absorb solar radiation. A Cary 5000 spectrometer was used to measurement. For the band gap calculation, the Kubelka-Munk method was utilized in the diffuse reflectance mode. The Kubelka-Munk Function is described by Myrick et al. 2011 [20] (equation 1), where *k* is the abortion coefficient and *s* is the scattering factor.

$$F(R) = (1\text{-}R)^2/2R = k/s \quad (1)$$

The band gap energy (Eg, eV) was obtained by extrapolation of the rising part of the curve to the x-axis (λg, nm), with calculation using: Eg = 1240/λg. Once the band gap is determined, it is possible to find the equivalent wavelength value (λeq), which is the minimum required energy for semiconductor activation related to the solar spectrum.

So it is possible to estimate the maximum wavelength that still contains sufficient energy to photo-excite electrons in the material, and thus estimate the percentage of the solar spectrum that the semiconductor is able to resort, and consequently its solar energy usage capacity.

In order to evaluate the morphology of the films, Scanning Electron Microscopy (SEM) studies were performed with a Carl Zeiss EVO MA10 instrument operated at 20 kV. Samples were gold-coated before starting the analysis and images were obtained in the secondary electron mode.

3. Results and discussion

3.1. Optical properties

The band gap analysis was performed with the purpose of determining the photo-activation energy of the films. The Kubelka-Munk Method was used with diffuse reflectance values. Figure 3 shows the diffuse reflectance spectrum of the samples and their band gap value (Eg).

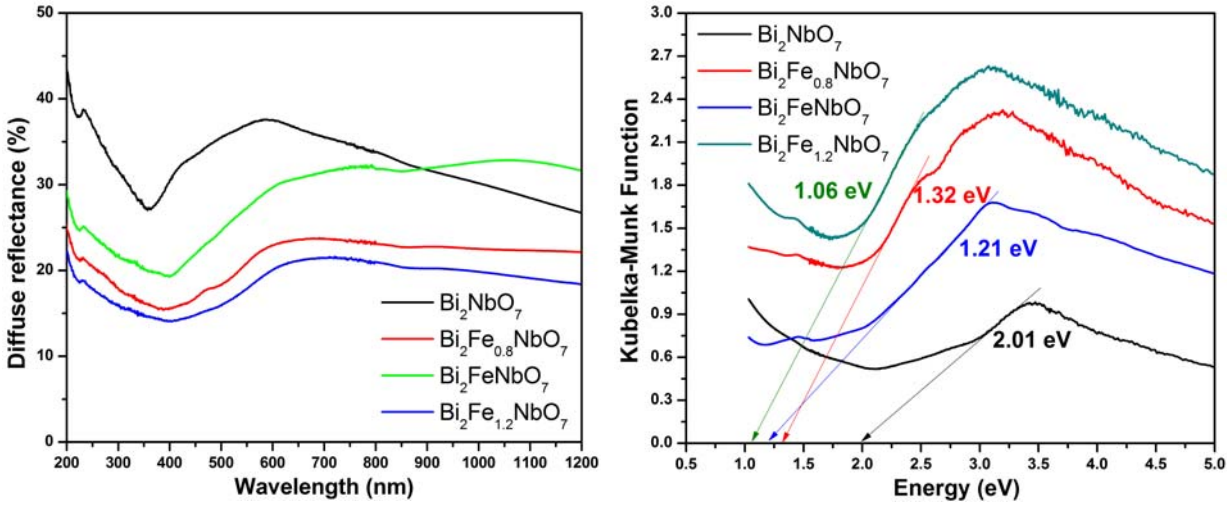

Figure 3. Diffuse reflectance and Kubelka-Munk function of the films.

All films presented semiconductor behaviour with Eg values lower than 2.01 eV. It is possible to observe a decreasing in the band gap value due the increasing of iron concentration. A linear regression was performed, identifying a first order polynomial with coefficient of determination (R^2) of 0.994, confirming a very strong relation between the increase of the amount of iron added and the decrease of the band gap value. One of the most consolidated explanations for this phenomenon claims that the adding of iron, which is a conductive material, produces intermediate energy levels between the valence and conduction band [21]. Then the material is able to absorb a larger part of the solar spectrum, since it requires photons with less energy to promote electrons from its valence band to conduction band. This phenomenon is known as red shift [22], and is accompanied by a change in the yellowish white colour of the film without iron to reddish in the highest concentration.

This higher light absorption capacity suggests a higher photo-catalytic activity. In addition, due to the effect of electrons and electron-holes in the electrical conductivity, lower values of band gap energy, due to the iron presence, could improve the electronic conductivity of the photo-electrodes, thus leading to a better electrical conductivity and ion transfer [23], which are desirable properties for photo-electrodes aiming water splitting. Table 1 summarizes the computed band gap values (Eg) and equivalent wavelengths (λeq) that are capable of providing enough energy for the activation of the photo-electrodes.

Table 1. Energy band gap values (Eg), Equivalent wavelengths (λ_{eq}) and solar spectrum usage percentage of the photo-electrodes.

$Bi_2Fe_xNbO_7$ x =	Band Gap (eV)	Equivalent wavelength (λ_{eq}) (nm)	Solar spectrum percentage (%) (AM1.5 Global) [24]
0	2.01	617	35.95
0.8	1.32	939	70.24
1.0	1.21	1025	75.36
1.2	1.06	1170	82.16

The radiation emitted by the sun is like that of a black body of 5,800 K. As it passes through the atmosphere, parts of sunlight are dispersed and/or absorbed. Chemical substances interact with sunlight and absorb certain wavelengths, altering the amount of light of those frequencies that reach the surface of the earth [25]. ASTM G-173 [24] formulates tables with values of energy quantity per wavelength (W m^{-2} nm^{-1}) that reaches the surface in normal plane (AM1.5 Direct), inclined plane (AM1.5 Global) and the irradiation before the atmospheric filter (AM0). Figure 4 shows the spectrum of solar radiation and equivalent wavelength (λeq) calculated from the optical band gap of the films.

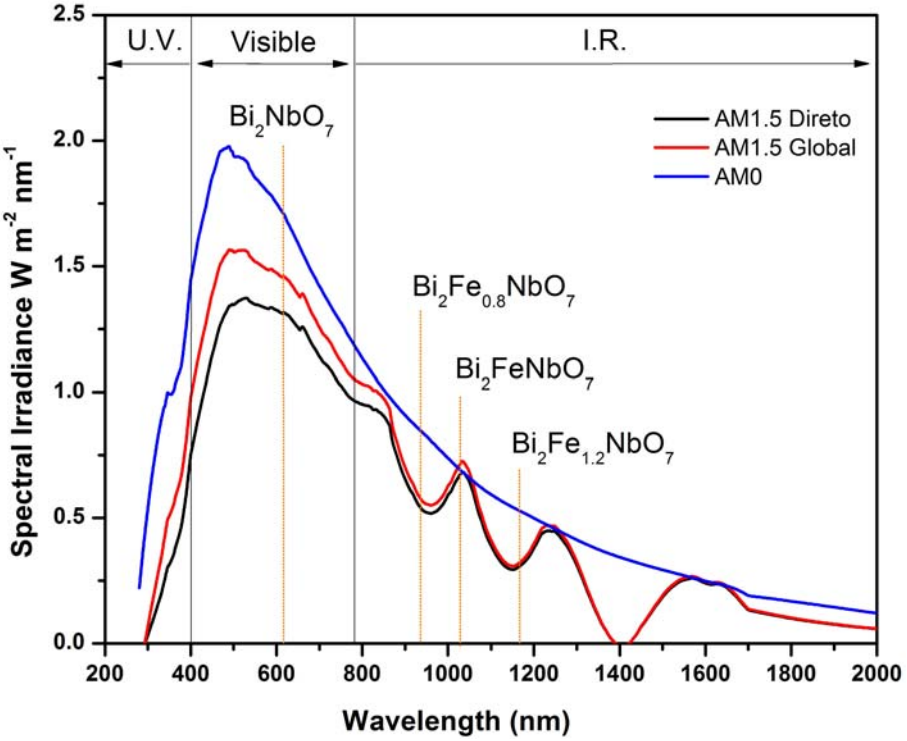

Figure 4. Spectral solar irradiance. Adapted from ASTM standard G-173-03 [24].

The lines corresponding to the equivalent wavelength (λeq) are represented for each film. It is important to emphasize that this is the maximum wavelength that still has enough energy to promote electrons from the valence band to the conduction band. Thus, the percentage of photons that have enough energy to activate the material can be obtained by the charge of the energy of all wavelengths smaller than the λeq. As shown in table 1, the films produced in this work can potentially be photo-excited by up to 82% of the solar spectrum that reaches the surface of the Earth, thus being a promising candidate for use as a photo-electrode for the hydrogen production by photo-electrolysis.

3.2. SEM studies

The morphology of mixed oxide films of $Bi_2Fe_xNbO_7$ was analyzed by Scanning Electron Microscope (SEM), and the results are shown in Figure 5. The micrographs on top show that the surface of the films is rough and with cracks distributed in all the analyzed area, characteristic from this kind of films [16,18]. Furthermore, these cracks are composed of particles with irregular size and shape. The film that does not contain iron (figure 5a, b) show fewer cracks and nanopores distributed by the shape, probably due to the exhaust gases during the heat treatment. This may be beneficial to the photo-electrolysis reaction by increasing the surface area of the film and thus the electrode-electrolyte interface [14].

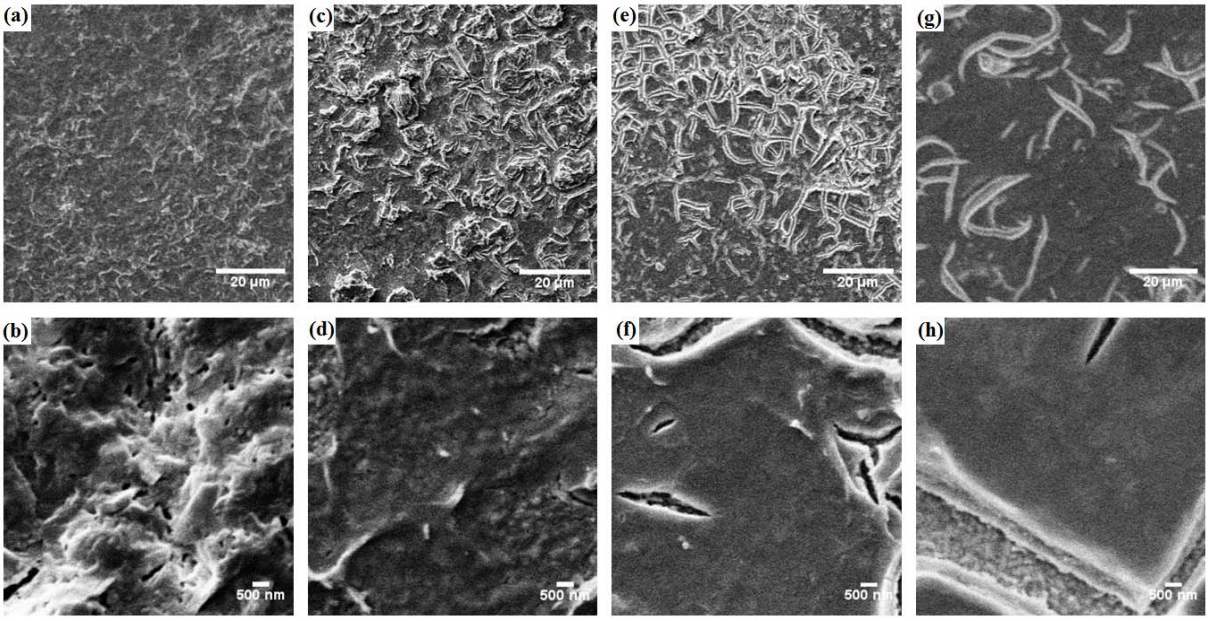

Figure 5. SEM micrographs of the films: **a, b)** Bi_2NbO_7; **c, d)** $Bi_2Fe_{0.8}NbO_7$; **e, f)** Bi_2FeNbO_7; **g, h)** $Bi_2Fe_{1.2}NbO_7$.

The films containing iron show progressive bigger cracks, it may have happened due the major amount of nitrates, its precursor. It is possible to observe that the increase in the concentration of iron causes a decrease in the amount of cracks and an increase in its size, on the other hand, the film surface is more homogeneous. In some cracks, it is possible to see the conductive layer of FTO.

Films deposited under substrates often develop tensile stresses large enough to cause cracking. A film heat treated at a high temperature and then cooled develops tensile stresses when the thermal expansion coefficient of the film exceeds that of the substrate. This is usually the case for oxides deposited on ceramic substrates, like FTO glass [26,27]. The cracked surface can be beneficial in the process of photo-electrolysis, mainly due to the greater surface area, directionality in the transport of electrons and the availability of electron-holes (h^+) for water oxidation [28]. However, if necessary, it is possible to manage the presence of cracks by changing the parameters of the heat treatment.

4. Conclusions

$Bi_2Fe_xNbO_7$ films were synthesized by an easy sol-gel route followed by heat treatment at relatively low temperature (600°C). The films exhibit a low band gap value and consequently an intense absorption of visible light. The increment of iron leads to a linear decrease in the band gap value. SEM studies show that the surface presents some cracks, possible due the presence of nitrates and residual tensile stresses. Further analyses should be performed to better understand their properties, however, based on data from UV-Vis spectroscopy and morphology studies, the photo-electrodes show high photo-catalytic activity under visible and even infrared light, which places them as potential

candidates for photo-anodes, being able to overcome the barrier that the low absorption of visible light imposes to the processes hydrogen production by photo-electrolysis.

Acknowledgment
This work was financially supported by the Brazilian National Council for the Improvement of Higher Education (CAPES). The present paper was presented inside the '*Toward a Sustainable Mobility*' special session as part of the '*Two Seats for a Solar Car*' research project, an action funded by the Italian Ministry of Foreign Affairs and International Cooperation within the Executive Programme of Cooperation in the field of Science and Technology between the Italian Republic and the Republic of Serbia.

References

[1] Harari Y N 2015 Sapiens - A Brief History of Humankind *An Animal of No Significance,* Harper
[2] Fuqiang Zhang L C 2019 Review and outlook of world energy development, *Non-Fossil Energy Development in China* (Elsevier) pp 1–36
[3] U.S. Energy Information Administration (EIA) 2016 International Energy Outlook, *U.S. Energy Inf. Adm.*
[4] Letcher T M (Trevor M . *Managing Global Warming : an Interface of Technology and Human Issues*
[5] United Nations department for economic and social Affairs 2019 *World Economic situation and prospects 2019* (UNITED NATIONS)
[6] Minak G, Brugo TM, Fragassa C, Pavlovic A, de Camargo FV and Zavatta N. 2019 Structural Design and Manufacturing of a Cruiser Class Solar Vehicl*e, J. Vis. Exp.* **143** *e58525*
[7] Minak G, Fragassa C and de Camargo F V 2017 A brief review on determinant aspects in energy efficient solar car design and manufacturing, International Conference on Sustainable Design and Manufacturing, Bologna, Italy, April 26 – 28, pp. 847-856
[8] *de Camargo F V, Giacometti M and Pavlovic A 2017 Increasing the energy efficiency in solar vehicles by using composite materials in the front suspension, International Conference on Sustainable Design and Manufacturing, Bologna, Italy, April 26 – 28, pp. 801-811*
[9] dos Santos K G, Eckert C T, De Rossi E, Bariccatti R A, Frigo E P, Lindino C A and Alves H J 2017 Hydrogen production in the electrolysis of water in Brazil, a review *Renew. Sustain. Energy Rev.* **68** 563–71
[10] Bak T, Nowotny J, Rekas M and Sorrell C 2002 Photo-electrochemical hydrogen generation from water using solar energy. Materials-related aspects, *Int. J. Hydrogen Energy* **27** 991–1022
[11] Zhu J and Zäch M 2009 Nanostructured materials for photocatalytic hydrogen production, *Curr. Opin. Colloid Interface Sci.* **14** 260–9
[12] Fujishima A and Honda K 1972 Electrochemical photolysis of water at a semiconductor electrode, *Nature* **238** 37–8
[13] Jang J S, Kim H G and Lee J S 2012 Heterojunction semiconductors: A strategy to develop efficient photocatalytic materials for visible light water splitting, *Catal. Today* **185** 270–7
[14] Ahmad H, Kamarudin S K, Minggu L J and Kassim M 2015 Hydrogen from photo-catalytic water splitting process: A review, *Renew. Sustain. Energy Rev.* **43** 599–610
[15] Ropero-Vega J L, Meléndez A M, Pedraza-Avella J A, Candal R J and Niño-Gómez M E 2014 Mixed oxide semiconductors based on bismuth for photoelectrochemical applications, *J. Solid State Electrochem.* **18** 1963–71
[16] Rosas-Barrera K L, Ropero-Vega J L, Pedraza-Avella J A, Niño-Gomez M E, Pedraza-Rosas J E and Laverde-Cataño D A 2011 Photocatalytic degradation of methyl orange using Bi_2MNbO_7 (M=Al, Fe, Ga, In) semiconductor film on stainless steel, *Catal. Today* **166** 135–9

[17] Ropero-Vega J L, Pedraza-Avella J A and Niño-Gómez M E 2015 Hydrogen production by photoelectrolysis of aqueous solutions of phenol using mixed oxide semiconductor films of Bi–Nb–M–O (M = Al, Fe, Ga, In) as photoanodes, *Catal. Today* **252** 150–6
[18] Ropero-Vega J L, Rosas-Barrera K L, Pedraza-Avella J A, Laverde-Cataño D A, Pedraza-Rosas J E and Niño-Gómez M E 2010 Photophysical and photocatalytic properties of Bi_2MNbO_7 (M = Al, In, Ga, Fe) thin films prepared by dip-coating, *Mater. Sci. Eng. B* **174** 196–9
[19] Bencina M, Valant M, Pitcher M W and Fanetti M 2014 Intensive visible-light photoactivity of Bi- and Fe-containing pyrochlore nanoparticles, *Nanoscale* **6** 745–8
[20] Myrick M L, Simcock M N, Baranowski M, Brooke H, Morgan S L and McCutcheon J N 2011 The Kubelka-Munk Diffuse Reflectance Formula Revisited *Appl. Spectrosc. Rev.* **46** 140–65
[21] Werapun U and Pechwang J 2019 Synthesis and Antimicrobial Activity of Fe:TiO_2 Particles, *J. Nano Res.* **56** 28–38
[22] Kumaravel V, Mathew S, Bartlett J and Pillai S C 2019 Photocatalytic hydrogen production using metal doped TiO_2: A review of recent advances, *Appl. Catal. B Environ.* **244** 1021–64
[23] Yousefipour K, Sarraf-Mamoory R and Yourdkhani A 2019 Iron-doping as an effective strategy to enhance supercapacitive properties of nickel molybdate, *Electrochim. Acta* **296** 608–16
[24] A.S.T.M. International 2012 ASTM G173-03(2012) *Stand. Tables Ref. Sol. Spectr. Irradiances Direct Norm. Hemispherical 37° Tilted Surf.*
[25] Lean J 2000 *Evolution of the Sun's Spectral Irradiance Since the Maunder Minimum* vol 27
[26] Xia Z C and Hutchinson J W 2000 Crack patterns in thin film, *J. Mech. Phys. Solids* **48** 1107–31
[27] Scharnberg A R A, Priebbnow A V, Arcaro S, Da Silva R M, Dos Santos P A M, Basegio T M and Rodriguez A A L 2019 Evaluation of the addition of soda-lime glass and yerba mate wastes in ceramic matrix, *Cerâmica* **65** 63–9
[28] Miklos D B, Remy C, Jekel M, Linden K G, Drewes J E and Hübner U 2018 Evaluation of advanced oxidation processes for water and wastewater treatment – A critical review, *Water Res.* **139** 118–31